

Stationary Frame Current Regulation of PWM Inverters with Zero Steady State Error

D. N. Zmood & D.G. Holmes

Department of Electrical and Computer Systems Engineering
Monash University
Wellington Road, Clayton, 3168
Australia

Abstract-- Current regulators for AC inverters are commonly categorised as hysteresis, linear PI or deadbeat predictive, with a further subclassification into stationary ABC frame and synchronous DQ frame implementations. Synchronous frame controllers are generally accepted to have a better performance than stationary frame controllers do, as they operate on DC quantities and hence can eliminate steady state errors. This paper establishes a theoretical connection between these two classes of regulators and proposes a new type of stationary frame controller, which achieves the same steady state performance as a synchronous frame controller. The new controller is applicable to both single phase and three phase inverters.

I. INTRODUCTION

Current regulation is an important issue for power electronic converters, and has particular application for high performance motor drives and boost type PWM rectifiers. Over the last few decades considerable research has been done in this area for voltage source inverters, and from this work three major classes of controller have evolved, i.e. hysteresis controllers, linear PI controllers and predictive controllers [1]. These classes can be further divided into stationary and synchronous d-q reference frame implementations by applying ac machine rotating field theory [2] [3]. Current controllers can be implemented in both analog and digital form for both stationary and synchronous reference frame systems.

In general, stationary frame controllers are regarded as less satisfactory for AC current regulation since they suffer from significant steady state amplitude and phase errors because of gain limitations at the reference fundamental frequency. In contrast, synchronous frame controllers act on DC signals and are therefore usually considered to be superior to stationary frame controllers since operation with zero steady state error is theoretically possible. However, a synchronous frame controller is more complex, and requires in particular a means of transforming a measured stationary frame AC current (or error) to rotating frame DC quantities, and transforming the resultant control action back to the stationary frame for execution. These transformations can introduce additional errors if the synchronous frame identification is not accurate.

In this paper, concepts taken from carrier-servo control systems [4] are used to develop a stationary frame current controller which achieves a similar steady state and transient performance as an equivalent synchronous frame controller.

The paper explores the relationship between stationary and synchronous frame controllers from a control system perspective, and shows how the controller transfer function can be transformed instead of the AC measured current error, to achieve a stationary frame linear PI current controller with zero steady state error. A significant advantage of this controller is its application to single phase current regulated systems, where synchronous frame transformations are more difficult to apply. The resultant controller is similar to that described in [5], but is more formally derived from control system theory and achieves a superior performance.

II. SERVO CONTROL SYSTEMS V'S HYBRID CONTROL SYSTEMS.

Servo control systems can be analysed using DC control system theory because the controlled quantity (or its integral) is DC under steady state conditions. Hence the steady state error for such controllers is determined by their open loop gain at DC, while their transient response is determined by the frequency response at the controller crossover frequency.

Figure 1 shows a block diagram for a typical DC motor position servo control system, where the forward path is composed of the DC controller compensation network - $H_{dc}(s)$, a saturating DC amplifier with gain K and a DC motor. Position feedback is commonly provided by a DC potentiometer.

In contrast for an AC control system such as a three phase current regulated VSI, the actuating and transducer signals are sinusoidal quantities.

With a stationary frame controller, the entire control loop operates on AC quantities, and is subject to steady state error as a consequence.

On the other hand, a synchronous frame controller contains signals which are both AC and DC, and hence can be considered as a hybrid control system.

The major difference between these two systems is the inclusion of a demodulator, which shifts the sidebands of the AC reference sinusoid in the stationary frame to the DC baseband region in the synchronous frame. Consequently, the controller compensation network can be implemented as a DC network, with its output signal being subsequently remodulated to re-introduce the reference frequency. The three phase d-q synchronous frame PI current regulator shown in Figure 2 is a good example of a hybrid control system.

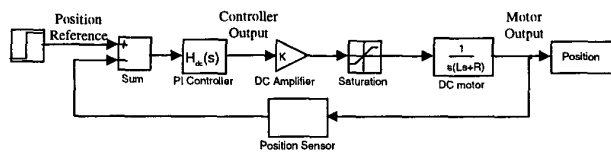


Figure 1: DC motor servo control system

Figure 3 shows typical open loop time and spectral response at various points along the block diagram of a DC servo system, and illustrates the lowpass filtering effects of the controller PI compensation network and the DC steady state nature of the system.

Figure 4 shows the open loop time and spectral response of a hybrid control system at a number of points along the block diagram. From this figure, it can be seen how the envelope of the amplitude modulated AC reference input exists in the frequency domain as sidebands about the fundamental reference frequency. (These sidebands contain the information which describes transient changes to the reference waveform with time.) The demodulation and remodulation effect of the synchronous frame transformation in converting these sidebands into a baseband frequency envelope in the synchronous frame can be clearly seen in Figure 4, together with the lowpass filtering effect of the synchronous frame controller DC compensation network.

Note that to prevent aliasing in the synchronous frame, the DC bandwidth within the controller must be limited to less than half that of the reference frequency to avoid the influence of the double reference frequency components caused by demodulation. In practice for the controllers considered in this paper, their open loop gain is small above this frequency range and this bandwidth limitation has minimal effect.

It is illuminating to also recognise that for the particular

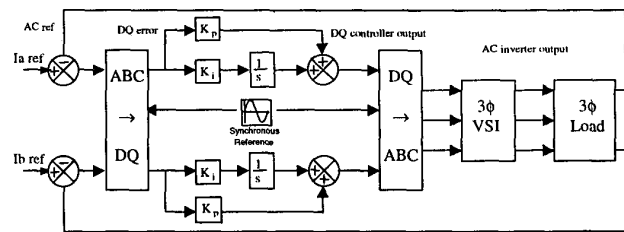


Figure 2: Hybrid synchronous frame control system

case of a three phase system using a stationary frame ABC to synchronous frame DQ transformation, the double carrier components of demodulation do not exist under steady state conditions as they sum to zero and leave only DC quantities to be operated on by the controller transfer function.

III. CONTROLLER COMPENSATION STRATEGIES

From servo control theory and the spectra of Figure 4, it can be proposed that if a transformation is done on the DC controller network of the stationary controller instead of demodulating the reference sideband signal spectra, the same control response as for a synchronous frame controller will be achieved without requiring the demodulation and modulation process. Essentially, the transformed controller directly operates on the AC error using sidebands about the reference fundamental.

Hence two approaches for control of an AC sinusoidally excited current controller can be considered.

A. Conventional Hybrid Compensation System

This type of controller has been well documented in the literature as a synchronous frame current controller, although it is usually not viewed from the perspective of frequency shifting the input reference spectrum to a DC baseband.

The advantage of this approach is that it allows the use of

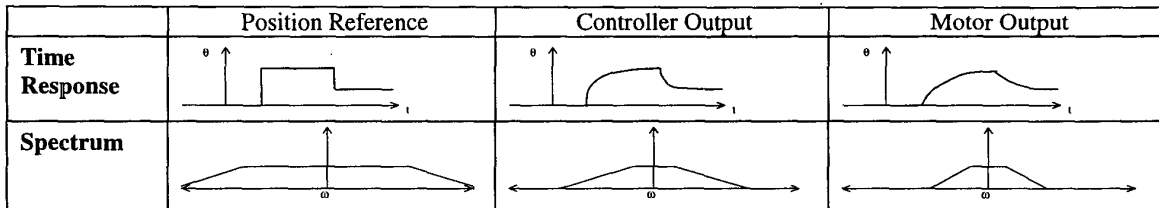


Figure 3: Time Response and Spectral range of signals within DC motor servo control system

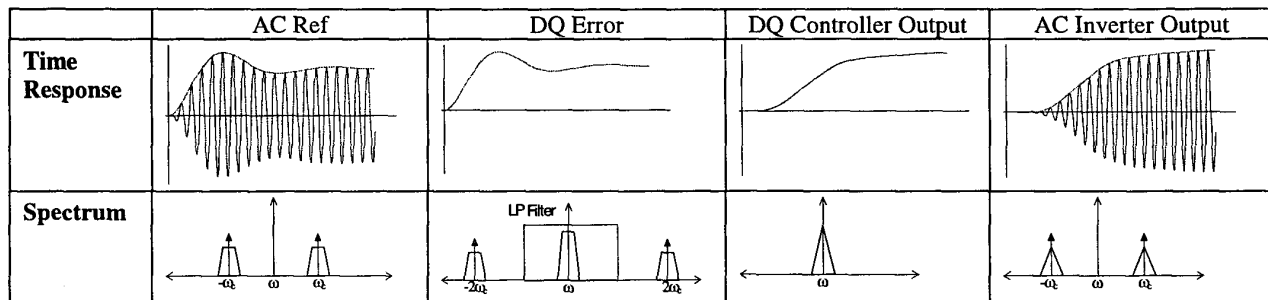


Figure 4: Time Response and Spectral range of signals within hybrid control system

well known DC compensation methods to develop the synchronous frame transfer function, and these are easier to design and construct than AC compensators. But the disadvantages are the additional complexity and computation required in adding a demodulator and modulator to the control system, and the need to develop an accurate synchronous frame reference signal. Also the application of this type of controller to single phase systems is not as straightforward as for three phase systems because of the double fundamental frequency components caused by the demodulation process.

B. Proposed AC Compensation System

This type of controller has not been recognised as applicable for power electronic systems, but is well known in control systems. The design strategy is to transform a desired DC compensation network into an equivalent AC compensation network, so that it has the same frequency response characteristic in the bandwidth of concern. The required exact transformation (developed in the Appendix) is

$$G_{AC}(s) = \frac{G_{DC}(s + j\omega) + G_{DC}(s - j\omega)}{2} \quad (1)$$

Unfortunately, physically realising the transfer function described in (1) is difficult. However, a suitable approximation for (1), when the reference signal bandwidth is small in comparison to the reference frequency itself, is to use the lowpass to bandpass technique developed in network synthesis, i.e.

$$G_{AC}(s) = G_{DC} \left(\frac{s^2 + \omega_c^2}{2s} \right) \quad (2)$$

The advantage of this approach is that the resultant controller requires much less signal processing than (1) and so is less sensitive to noise. Furthermore, the application of this technique to single phase systems is straightforward and undifferentiated from its application to three phase systems. But the approach does have the disadvantage for variable frequency applications where the resonant frequency of the AC compensator must be shifted in accordance with the required output fundamental. However, this problem is no more challenging than the need to maintain a synchronous reference transformation which follows a varying fundamental frequency.

IV. REALISATION OF THE NEW AC COMPENSATION SYSTEM

A major objective for AC current controllers is to achieve zero phase and magnitude error. Using AC Compensation, this objective can be achieved by transforming a DC

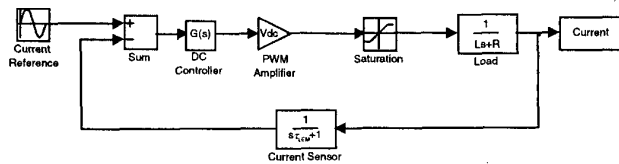


Figure 5: Model of a current regulated PWM inverter

compensator that achieves this goal into an AC compensator, which will have the same performance in AC control systems.

Figure 5 shows a typical DC compensated current regulation system, where for convenience the asymmetrically modulated PWM converter stage has been modelled as a simple saturating gain.

For DC, a conventional PI compensator achieves the desired zero steady state error. Using the lowpass to bandpass transformation (2), an equivalent AC compensator would therefore have an open loop transfer function of:

$$G_{DC}(s) = K_P + \frac{K_I}{s} \quad (3a)$$

$$G_{AC}(s) = K_P + \frac{2K_I s}{s^2 + \omega_c^2} \quad (3b)$$

which has a frequency and phase response shown in Figure 6.

The closed loop transfer function for the linear model of Figure 5 with this compensator is given by,

$$T(j\omega) = \frac{G_{AC}(j\omega) V_{DC} e^{-j\omega\tau}}{R + sL + G_{AC}(j\omega) V_{DC} e^{-j\omega\tau}} \quad (4)$$

From (4), the closed loop transfer function of the system will clearly approach unity at the fundamental reference (target) frequency with no phase or magnitude error in the output waveform. However, there are two major problems with this implementation. Firstly it implies a network with an infinite Q which is not realisable in either digital or analog form. Secondly, any slight displacement between the reference frequency and the filter network resonant frequency would lead to a decline in performance. But a more practical compensator that approximates this ideal network is given by:

$$G_{DC}(s) = K_P + \frac{K_I \cdot \omega_{cut}}{s + \omega_{cut}} \quad (5a)$$

$$G_{AC}(s) = K_P + \frac{2K_I \omega_{cut} s}{s^2 + 2\omega_{cut} s + \omega_c^2} \quad (5b)$$

where ω_{cut} is the lower breakpoint frequency of the DC transfer function. This network has a frequency and phase response as shown in Figure 7.

The steady state output phase and magnitude error achieved by this compensator can now be determined by the magnitude and phase response of the closed loop transfer function at the modulation carrier frequency.

V. STABILITY CONSIDERATIONS

The significance of (5a) is that linear control theory can be used to investigate the stability of the new controller using the linear model shown in Figure 5. Using conventional Bode plots, it is straightforward to show that the controller integral gain can be made sufficiently large to essentially remove all steady state error (similar to the effect of the finite integral gain that most practical DC compensators can achieve), without any significant stability limitations.

Note: The current sensor was modelled by a single pole lowpass filter with breakpoint at 100Khz. This component has

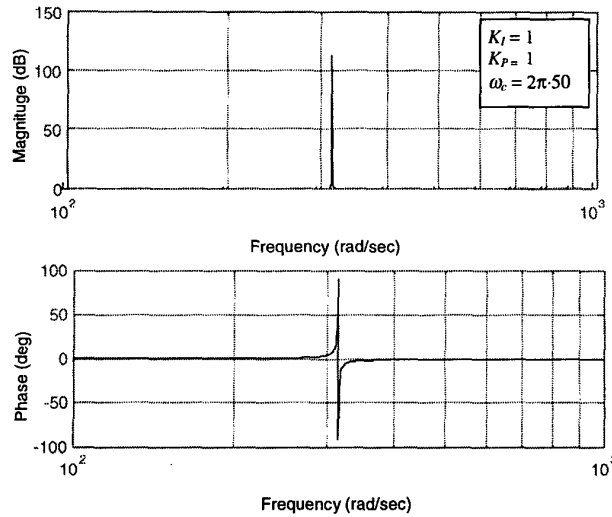


Figure 6: Bode Plot of AC Compensator from Equation (3b),

little effect on the magnitude response of the system but the additional phase it introduces can have a significant effect on the system stability.

Resonant controllers provide very little gain outside their bandpass region due to their narrowband frequency response. Hence, to achieve a reasonable transient response a proportional term is also required. Figure 8 shows the magnitude and phase bode diagrams for a simple proportional controller and the two controllers described by (3b) and (5b). For $K_P=0.1$ the magnitude crossover frequency (ie. controller gain becomes less than 1) of the simple proportional controller occurs at 3kHz, as indicated in Figure 8. The phase plot shows a phase margin of more than 100 degrees at this frequency so the system is clearly stable.

The introduction of the resonant controller terms radically alters the Bode plots at the resonant frequency but has little effect at the crossover frequency for the controller parameters

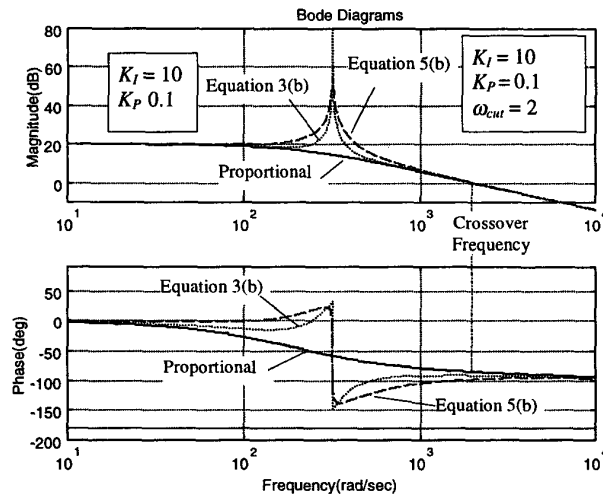


Figure 8: Open Loop Bode Plots of Proportional and Resonant Controllers

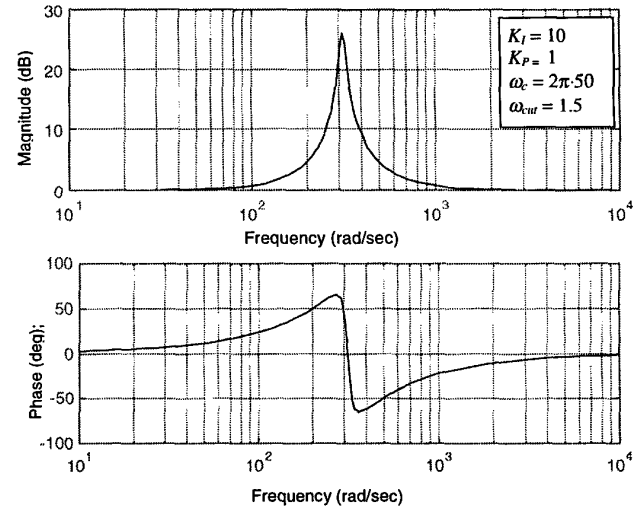


Figure 7: Bode Plot of AC Compensator from Equation (5b),

chosen. Hence, both resonant controllers remain stable below the crossover frequency because the phase is always less than 180° . Figure 8 also shows that most of the high frequency or transient response of the controller is determined by the proportional gain since the controller magnitude response returns to that of a simple proportional system at higher frequencies. So, the larger the proportional gain the faster will be the transient response.

This suggests a simple two step design procedure for the complete controller. Firstly, chose a proportional gain such that the controller is stable and gives a good transient response. Then design a resonant component that gives the desired steady state phase and amplitude error without making the phase margin too small.

C. Effect of the Quality Factor (Q)

One attraction of the lossy resonant compensator is its ability to control the quality factor (Q) of the response. In signal theory the Q of a second order system is given by,

$$Q = \frac{\omega_c}{\omega_2 - \omega_1} = \frac{\omega_c}{2\omega_{cut}} \quad (6)$$

where: ω_c is the centre frequency

ω_1, ω_2 are the two 3dB frequencies

The Q of a circuit determines the bandwidth of the filter network. Therefore by lowering Q , the system can be made less sensitive to variations in the fundamental frequency or the controller realisation. However, the consequence is that lowering the Q spreads the frequency response of the circuit, which means that the effect of the resonant term at the crossover frequency will be more significant.

Figure 9 illustrates how the reference frequency bandwidth widens while the phase margin of the resonant controller is degraded as Q is decreased. However, since the phase response never exceeds 180° , the controller remains stable. This offers potential to gain an improved response with a

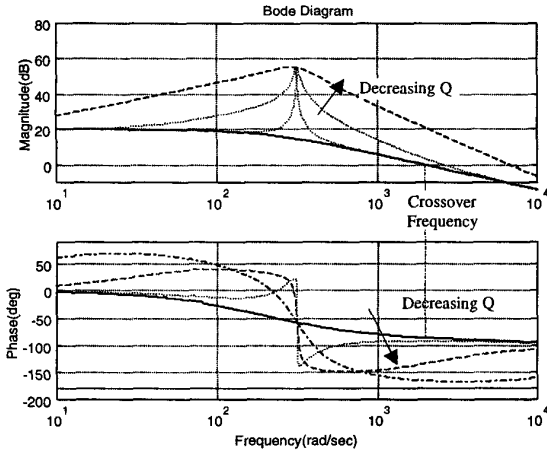


Figure 9: Open Loop Bode Plot for variations in Q

varying frequency reference input without having to modify the filter network. This issue is not explored further in this paper because of space considerations.

D. PWM Constraint

A fundamental constraint of PWM systems is that the maximum rate of change of the reference should not equal or exceed that of the carrier signal or for digital systems the maximum frequency of the reference should be less than half the sample frequency. For an analog system this requirement must be met for a fixed PWM switching frequency. For the simple proportional feedback system given in Figure 5 and an analog sine-triangle PWM system, the critical gain is:

$$K_p(\max) = \frac{4Lf_{carrier}}{V_{DC}} \quad (7)$$

If the load is purely resistive a lowpass filter can be placed after the current sensor or as part of the compensator to restrict the rate of change of the error signal.

A further constraint exists for a regular sampled PWM system which can introduce a phase delay into the inverter output. It is anticipated that conventional digital systems control theory can be used to investigate this issue, but this is left for a future investigation to pursue.

VI. SIMULATION AND EXPERIMENTAL RESULTS

Figure 10 shows the simulated steady state and transient response that can be achieved with the new controller for both a low and a high backemf load. Table I defines the controller parameters for these results (and also the previous stability simulations). In both cases it can be seen that there is no steady state error during continuous modulation, and only a slight error just after the transient event occurs. This error is caused by the settling time of the resonant part of the controller transfer function.

Figure 11 presents results from an experimental system driving an R-L load, where it can be seen that a very similar response has been obtained. This confirms the effectiveness

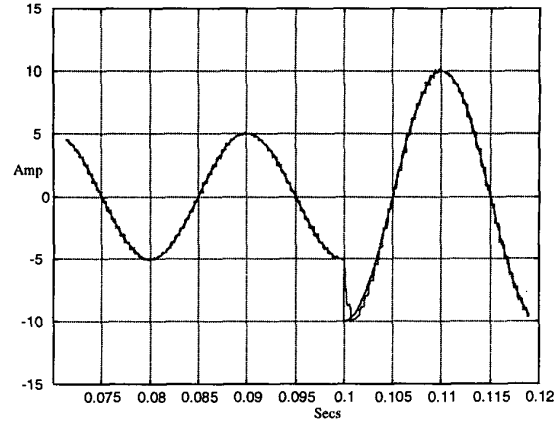


Figure 10a : Simulated Response of AC Compensator, zero backemf

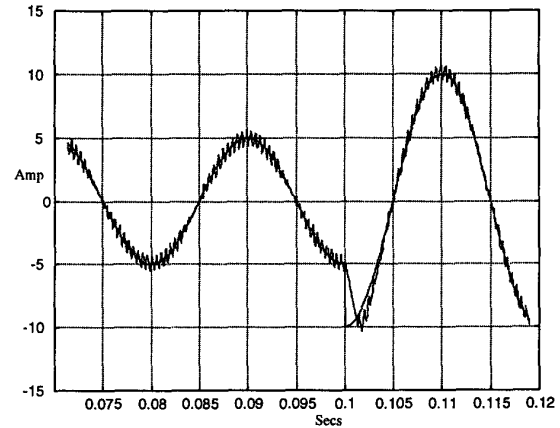


Figure 10b: Simulated Response of AC Compensator, 0.7pu backemf

of the new controller. Note in particular that this controller is equally effective for single or three phase systems, since it does not rely on a synchronous frame d-q transformation.

Figure 12 shows the simulated response for a three phase system using stationary resonant PI controllers on two phases (the third phase inverter output is made equal to minus the sum of the other two phases for reduced complexity).

VII. SUMMARY

Synchronous frame current regulators are usually accepted as being superior to stationary frame controllers because the synchronous transformation of the AC current error allows conventional DC compensation strategies to be used to achieve zero steady state error. In this paper, the advantage is

LOAD	Inductance	5 mH
	Resistance	2 Ohms
Supply Volts		200 Vdc
Controller Gains	Proportional	0.1
	Resonant	10
Switching Freq		1 kHz

Table I: Simulation & Experimental Parameters

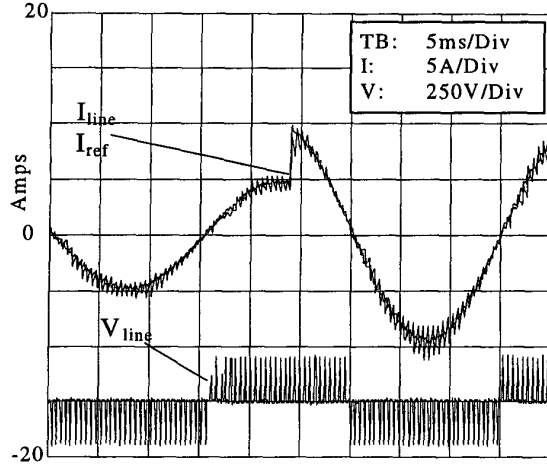


Figure 11 : Experimental Response of AC Compensator, zero backemf

shown to derive from the carrier demodulation process inherent in the synchronous transformation.

Using this concept, it is then shown how a stationary frame current regulator with almost equivalent performance can be achieved by transforming the controller compensation network rather than the current error signal. The result is a stationary frame current controller that achieves zero steady state error, and is equally applicable to single phase or three phase systems. The new controller has been fully evaluated both in simulation and experimentally.

VIII. REFERENCES

- [1] M. P. Kazmierkowski and M. A. Dzieniakowski, "Review of Current Regulation Techniques For Three-Phase PWM Inverters", Conference Record.IECON '94, pp. 567 - 575, 1994
- [2] T. M. Rowan and R. J. Kerkman, "A New Synchronous Current Regulator and an Analysis of Current Regulated PWM Inverters", IEEE Transactions on Industry Applications, Vol. IA-22, No. 4, pp. 678 - 690, 1986
- [3] Y. Sato, T. Ishizuka, K. Nezu, and T. Kataoka, "A New Control Strategy for Voltage-Type PWM Rectifiers to Realise Zero Steady-State Control Error in Input Current", IEEE Transactions on Industry Applications, Vol. 34, No. 3, pp. 480 - 486, 1998
- [4] J.J. D'Azzo and C.H. Houpis, "Feedback and Control System Analysis and Synthesis", 2nd Edn., McGraw-Hill, 1966
- [5] Yukihiko Sato, et.al., "A New Control Strategy for Voltage-Type PWM Rectifiers to Realise Zero Steady-State Control Error in Input Current", Vol 34., No. 3, pp. 480-486, May 1998.

APPENDIX: DEVELOPMENT OF AC TRANSFORMATION

Consider two equivalent controllers, one operating on DC quantities and the other on AC quantities. Assume that the reference signals are bandlimited to less than the fundamental frequency. Then the controller transfer functions are given by:

$$\begin{aligned} V_{DC}(s) &= E_{DC}(s)H_{DC}(s) \\ V_{AC}(s) &= E_{AC}(s)H_{AC}(s) \end{aligned} \quad (A.1)$$

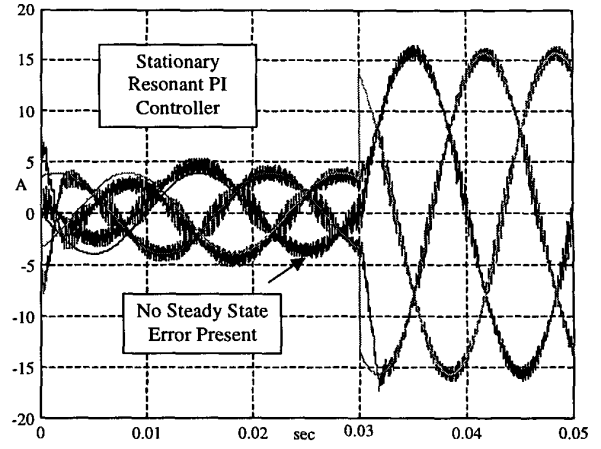


Figure 12: Simulation Response of Three Phase AC Compensator

In the time domain these functions become,

$$\begin{aligned} v_{DC}(t) &= e_{DC}(t) \otimes h_{DC}(t) \\ v_{AC}(t) &= e_{AC}(t) \otimes h_{AC}(t) \end{aligned} \quad (A.2)$$

where \otimes denotes a convolution product.

The relationship between the time domain DC and AC quantities is given by,

$$\begin{aligned} v_{AC}(t) &= v_{DC}(t) \cos(\omega t) \\ v_{DC}(t) &= 2v_{AC}(t) \cos(\omega t) \end{aligned} \quad (A.3)$$

Note: The factor of two in the above relationship is to maintain the energy of the DC portion of the signal after the demodulation process.

So using (10), and substituting from (11) gives:

$$\begin{aligned} v_{AC}(t) &= [e_{DC}(t) \otimes h_{DC}(t)] \cos(\omega t) \\ &= 2[e_{AC}(t) \cos(\omega t) \otimes h_{DC}(t)] \cos(\omega t) \end{aligned} \quad (A.4)$$

Taking the Laplace Transform and using the frequency convolution theorem gives:

$$\begin{aligned} V_{AC}(s) &= 2[H_{DC}(s) \cdot L\{e_{AC}(t) \cos(\omega t)\}] \otimes \frac{s}{s^2 + \omega^2} \\ &= \left[\begin{matrix} H_{DC}(s + j\omega)E_{AC}(s) \\ + H_{DC}(s - j\omega)E_{AC}(s) \end{matrix} \right] \otimes \frac{s}{s^2 + \omega^2} \end{aligned} \quad (A.5)$$

Applying the frequency convolution leads to:

$$V_{AC}(s) = \left[\begin{matrix} H_{DC}(s + j\omega)E_{AC}(s + 2j\omega) + \\ H_{DC}(s - j\omega)E_{AC}(s) + \\ H_{DC}(s + j\omega)E_{AC}(s) + \\ H_{DC}(s - j\omega)E_{AC}(s - 2j\omega) \end{matrix} \right] \otimes \frac{s}{s^2 + \omega^2} \quad (A.5)$$

The system is assumed to be bandlimited to less than the fundamental/carrier frequency, so that:

$$E_{AC}(s + 2j\omega) = E_{AC}(s - 2j\omega) = 0 \quad (A.6)$$

and hence,

$$H_{AC}(s) = \frac{1}{2}[H_{DC}(s + j\omega) + H_{DC}(s - j\omega)] \quad (A.7)$$